International Journal of Science and Research (IJSR)
ISSN (Online): 2319-7064
Impact Factor (2012): 3.358

Synergism between N, N-dimethyl-2-(phenyl (o-tolyl)methoxy)ethanamine and Iodide Ions on the Corrosion of Carbon Steel in 1 M HCl

Ahmed A. Farag[1], I. M. Ibrahim[2]

[1]Additives Laboratory, Petroleum Applications Department, Egyptian Petroleum Research Institute (EPRI)
1 Ahmed El-Zomor St., Nasr City, 11727, Cairo, Egypt

[2]Asphalt Laboratory, Petroleum Applications Department, Egyptian Petroleum Research Institute (EPRI)
1 Ahmed El-Zomor St., Nasr City, 11727, Cairo, Egypt

Abstract: ***Corrosion inhibition of carbon steel in 1 M HCl by N,N-dimethyl-2-(phenyl(o-tolyl)methoxy)ethanamine (DPTA), in the absence and presence of iodide ions was investigated using weight loss, potentiodynamic polarization and electrochemical impedance spectroscopy techniques. The results revealed that DPTA inhibit the steel corrosion and the inhibition increases by increasing its concentration and increases further by the addition of iodide ions. The adsorption of DPTA on the carbon steel surface was found to obey Langmuir adsorption isotherm. Synergism parameters (S) are more than unity indicates that the enhanced inhibition efficiency in the presence of iodide ions is only due to synergism.***

Keywords: Corrosion inhibitor, Diphenhydramine, Carbon Steel, Synergism, Iodide ion, Adsorption.

1. Introduction

Acid solutions are generally used for acid pickling, industrial cleaning, acid descaling, oil-well acidizing in oil recovery and the petrochemical processes. Aqueous solutions of acids are among the most corrosive media. So, the corrosion rate at which metals are destroyed in acidic media is very high, especially when soluble corrosion products are formed [1–5]. The most used corrosion inhibitors are organic compounds which tend to decrease the corrosion rate of iron in acid solutions. The most of effective organic inhibitors that contain heteroatom such as O, N, S, and multiple bonds in their molecules through which they are adsorbed on the metal surface [6−9].

Although heterocyclic organic compounds have good anti-corrosive activity; they are highly toxic to both human beings and the environment. The health issues, cost and environmental regulatory restrictions have made researchers focus on the development of non-toxic corrosion inhibitors [10,11]. As an important heterocyclic compound, diphenhydramine and its derivatives is non-toxic and biodegradable; this makes the investigation of their inhibiting properties significant within the context of the current priority to produce eco-friendly inhibitors [12]. The selection of N,N-dimethyl-2-(phenyl(o-tolyl)methoxy)ethanamine($C_{18}H_{23}NO$) as a corrosion inhibitor is based on: (a) non-toxicity (b) contain two aromatic rings, electronegative oxygen and nitrogen atom as active centers through which they can easily adsorb on the metal surface. Synergism is an effective approach to reduce the dosage of organic inhibitors and to diversify the application of the inhibitors in acidic media [13]. This synergism has been reported to be due to the increased surface coverage as a result of ion–pair interactions between an organic cation and the halide anion. Halide ion presents in an inhibiting solution firstly adsorbs on the corroding surface by creating oriented dipoles and thus it facilitates the adsorption of inhibitor cations on the dipoles [14]. As reported in the literature the synergism order in the presence of different halides is $I^- > Br^- > Cl^-$. Due to its larger size and ease polarizability, iodide ions can easily adsorb on metal surface and provide better synergistic effect [15]. In the present work, the synergistic inhibition between iodide ions and a new non-toxic corrosion inhibitor, N,N-dimethyl-2-(phenyl(o-tolyl)methoxy)ethanamine

(DPTA) in 1 M HCl is investigated by potentiodynamic polarization, electrochemical impedance spectroscopy and weight loss spectra (EIS) techniques. The interaction of iodide ions with the DPTA molecule and its synergism towards the inhibition of acid corrosion of carbon steel is discussed.

2. Materials and methods

2.1. Materials

The used inhibitors DPTA and KI were obtained from Sigma–Aldrich and used as received. The chemical structure of DPTA is given in Figure 1. The chemical composition of the carbon steel used as the following (wt.%): 0.07% C, 0.24% Si, 1.35% Mn, 0.017% P, 0.005% S, 0.16% Cr, 0.18% Ni, 0.12% Mo, 0.01% Cu and the remainder Fe.

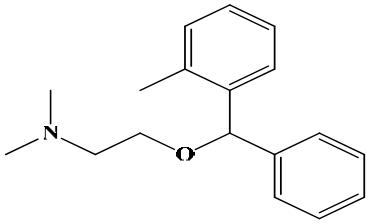

Figure 1: Molecular structure of DPTA

2.2. Preparation of samples and solutions

The carbon steel specimens were carefully abraded by different grades of emery paper (up to 1200 grit) and subsequent cleaning with distilled water and acetone. The corrosive solution of 1 M HCl was prepared by dissolving analytical grade, 37% HCl in distilled water. The corrosion tests were performed in 1 M HCl in the absence and presence of various concentrations of investigating inhibitors. The inhibitors solutions were prepared in 1 M HCl. For each experiment, a freshly prepared solution was used under air atmosphere without stirring at room temperature.

2.3. Electrochemical measurement procedure

A three-electrode corrosion cell (volume 100 ml) was used for the electrochemical measurements under static aerated conditions in laboratory room temperature. The experiments were performed using Volta lab 40 (Tacussel-Radiometer PGZ301) potentiostate and controlled by Tacussel corrosion analysis software model (Voltamaster 4). The carbon steel working electrode was aligned vertically with area 1cm^2 exposed to the solution. A platinum and saturated calomel electrode (SCE) electrode was used as the counter and a reference electrode, respectively. The working electrode was immersed in the test solution for 30 minutes to a establish steady state open circuit potential (E_{ocp}). After measuring the E_{ocp}, the electrochemical measurements were performed. The EIS experiments were conducted in a frequency range with high limit of 10^5 Hz and different low limit 10^{-2} Hz with an amplitude of 10 mV peak-to-peak using ac signals at open circuit potential. The polarization curves were obtained in the potential range from −900 to −200 mV(SCE) with 1 mV s^{-1} scan rate. To achieve a reproducibility three parallel experiments were performed for each test.

2.4. Weight loss measurements

Weight loss experiments were carried out using carbon steel coupons specimens having dimensions of 7.0 cm × 2.0 cm × 0.3 cm. After abraded and cleaning the specimens were accurately weighted and then immersed in 1 M HCl solution with and without various concentrations of the investigated inhibitors. After 24 h exposure, the specimens were taken out, rinsed thoroughly with distilled water, dried and weighted accurately. Three parallel experiments were performed for each test to achieve the reproducibility. The average weight loss, ΔW (mg) was calculated using the following equation [16]:

$$\Delta W = W_1 - W_2 \quad (1)$$

where W_1 and W_2 are the average weight of specimens before and after exposure, respectively.

3. Results and Discussion

3.1. Electrochemical impedance spectroscopy

The electrochemical impedance measurements were undertaken to provide information about the kinetics of electrochemical processes on the carbon steel/aggressive solution interface, and how this is modified in the presence of investigating inhibitors.

Figures 2 & 3 show Nyquist plots of carbon steel in 1 M HCl in the absence and presence of various concentrations of DPTA and its mixture with KI, respectively; while the Bode plots of DPTA were given in Figure 4.

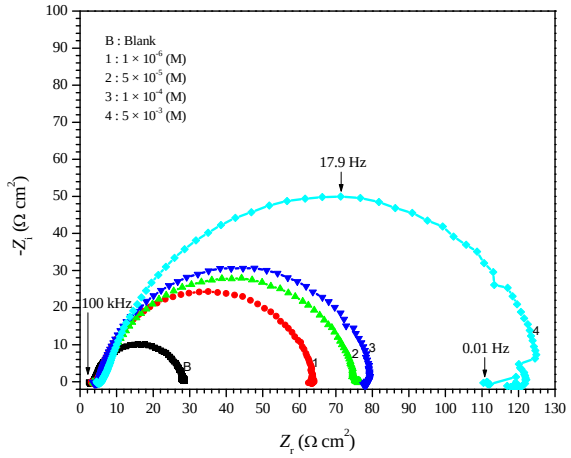

Figure 2: EIS for carbon steel electrode obtained in 1 M HCl solution and containing various concentrations of DPTA

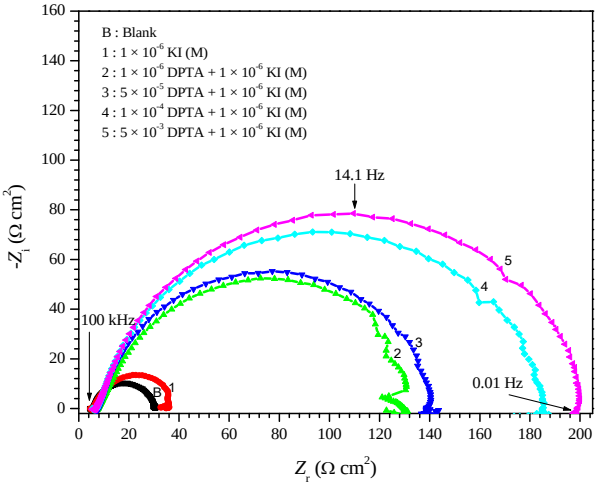

Figure 3: EIS for carbon steel electrode obtained in 1 M HCl solution and containing various concentrations of DPTA/KI

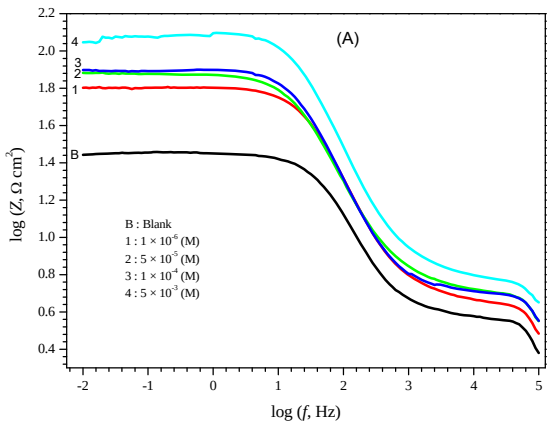

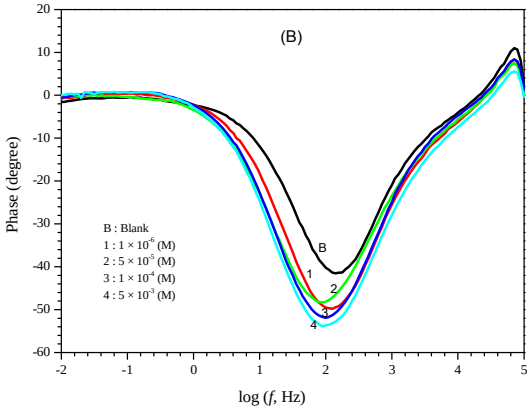

Figure 4: (a) Bode impedance plots of logZ vs. Hz and (b) Bode-phase angle plots vs. Hz for carbon steel electrode in 1 M HCl solution and containing various concentrations of DPTA

Table 1: Impedance parameters derived from the Nyquist plots for carbon steel in 1M HCl solution in the absence and presence of investigated inhibitors

DPTA Conc. (M)	KI Conc. (M)	R_s (ohm.cm²)	R_{ct} (ohm.cm²)	C_{dl} (μF.cm^{-2})	η_i (%)
0	0	3.6	24.8	128.1	–
1×10^{-6}	0	4. 7	59.1	53.8	58.0
1×10^{-5}	0	5.3	70.4	45.2	64.7
1×10^{-4}	0	5.2	73.7	43.2	66.3
1×10^{-3}	0	7.0	115.2	27.7	78.4
0	1×10^{-6}	4.5	27.0	109.0	08.1
1×10^{-6}	1×10^{-6}	5.1	120.7	26.4	79.4
1×10^{-5}	1×10^{-6}	7.4	131.3	24.2	81.1
1×10^{-4}	1×10^{-6}	7.9	174.9	18.2	85.8
1×10^{-3}	1×10^{-6}	7.1	189.5	16.8	86.9

Table 1 shows the EIS parameters obtained from Nyquist plots (R_s, the solution resistance, R_t, the charge transfer resistance, C_{dl}, the double layer capacitance, and η_i, the inhibition efficiency). R_t values were calculated from the difference in the impedance at lower and higher frequencies. The inhibition efficiency can be calculated from the following equation [17]:

$$\eta_i = \left(\frac{R_t - R_t^o}{R_t} \right) \times 100 \quad (2)$$

where R_t and R_t^o are the charge transfer resistance in the presence and absence of the inhibitors, respectively. The values of C_{dl} were calculated at the frequency f_{max}, at which the imaginary component of the impedance is, maximal ($-Z_{max}$) by the following equation [18]:

$$C_{dl} = \frac{1}{2\pi f_{max} R_t} \quad (3)$$

The thickness of the protective layer is related to the double layer capacitance according to Helmholtz model [19]:

$$C_{dl} = \frac{\varepsilon_o \varepsilon}{d} A \quad (4)$$

where ε_o is the permittivity of free space (8.854×10^{-12} Fm^{-1}), ε the local dielectric constant, d the thickness of the film and A is the surface area of the electrode. In fact, the decrease in C_{dl} values can result from a decrease in local dielectric constant and/or an increase in the thickness of the electrical double layer. It could be assumed that the decrease of C_{dl} values is caused by the gradual replacement of water molecules by adsorption of inhibitor molecules on the electrode surface, which decreases the extent of the metal dissolution [20].

Nyquist plots reported in Figures 2 & 3 have been almost always very simple, similar to a semicircle for all systems over the frequency range studied. The high frequency intercept with the real axis is assigned to the solution resistance (R_s), the low frequency intercept being ascribed to the transfer resistance (R_t). The semicircle actually corresponds to one time constant process as, even resulted in the Bode phase plots (Figure 4).

By inspection results in Figure 2, it can be noted that the increase R_t diameter in the presence of DPTA with respect to those obtained in blank solution (without inhibitors). Moreover, the increase in diameter with increase DPTA concentration indicates that the amount of adsorbed inhibitor molecules on the electrode surface is increased. The adsorbed DPTA molecules form a protective layer on the carbon steel surface which isolates the metal from dissolution and charge transfer process [21]. As the concentration of DPTA increases, the inhibition efficiency (η_i) also increases, but the extent of increase in η_i is less (78.4%) at DPTA concentration 1×10^{-3} M. In order to enhance the corrosion inhibition performance of DPTA in 1 M HCl solution, the synergism study with iodide ions was undertaken. Figure 3 shows that the inhibition efficiency increases by addition of small concentration (1×10^{-6} M) of KI to different concentration of DPTA inhibitor molecules. Although the inhibition efficiency of 1×10^{-6} M KI alone is 5.7% of the carbon steel in 1 M HCl solution, but the combination of 1×10^{-6} M KI and 1×10^{-3} M DPTA, raise the inhibition efficiency for to 86.9% as given in Table 1. This indicates a synergistic effect between DPTA and KI. Bode plots in absence and presences of DPTA are given in Figure 4. In the high frequency region the log$Z$ values tend to become zero (Figure 4A) with increasing frequency and the phase angle values go rapidly towards 0° (Figure 4B). This is a response of resistive behavior and corresponds to the solution resistance R_s. In the intermediate frequency region, a linear relationship between log$Z$ vs. log f with a slope near −1 and the phase angle approaching −60° has been observed. This is a characteristic response of capacitive behavior at intermediate frequencies. An ideal capacitive response would result in a slope of −1 and a phase angle of −90°; but in an electrochemical system generally ideal behavior does not obtain [22].

The impedance spectra for the Nyquist plots were analyzed by fitting to the equivalent circuit model shown in Figure 5, which has been used previously to model the steel/acid interface [23].

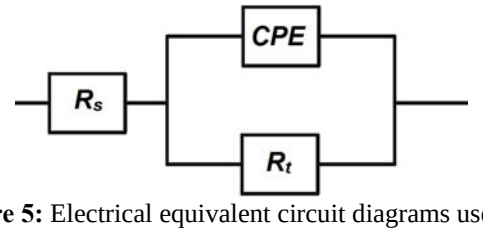

Figure 5: Electrical equivalent circuit diagrams used for modeling, metal/solution interface

The circuit comprises a solution resistance R_s shorted by a constant phase element (CPE) that is placed in parallel to the charge transfer resistance R_{ct}. The value of the charge transfer resistance is indicative of electron transfer across the interface. The use of the CPE has been extensively described in the literature [24] and is employed in the model to compensate for the inhomogeneities in the electrode surface as depicted by the depressed nature of the Nyquist semicircle. The introduction of such a CPE is often used to interpret data for rough solid electrodes. The impedance, Z, of the CPE is [25]:

$$Z_{CPE} = \left[Q(j\omega)^n\right]^{-1} \quad (5)$$

where the coefficient Q is a combination of properties related to different physical phenomena like surface inhomogeneousness, electro-active species, inhibitor adsorption, porous layer formation, etc., j is an imaginary number ($j^2 = -1$), ω is the angular frequency ($\omega = 2\pi f$) and the exponent n has values between −1 and 1. A value of −1 is a characteristic for an inductance, a value 1 corresponds to a resistor, and a value of 0.5 can be assigned to diffusion phenomenon [26].

3.2. Polarization curve

The polarization curves for carbon steel in 1 M HCl with and without various concentrations of the DPTA and combination of DPTA/KI were shown in Figures 6 & 7, respectively. The parameters extracted from the polarization curve as: corrosion potential E_{corr}, corrosion current density i_{corr}, anodic Tafel slopes β_a, cathodic Tafel slopes β_c and inhibition efficiency (η_t) were gained and listed in Table 2. The inhibition efficiency was calculated as follows [27]:

$$\eta_t = \left(\frac{i_t - i_t^o}{i_t}\right) \times 100 \quad (6)$$

where i and i^o are uninhibited and inhibited corrosion current densities, respectively. It could be seen from Table 2 that the i_{corr} values decrease considerably in the presence of DPTA and decreased with increasing its concentration.

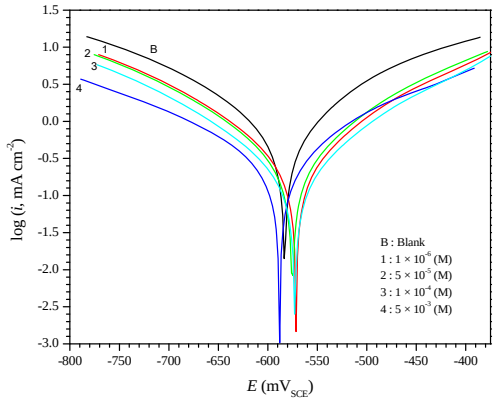

Figure 6: Polarization curves for carbon steel obtained in 1 M HCl solution and containing various concentrations of DPTA

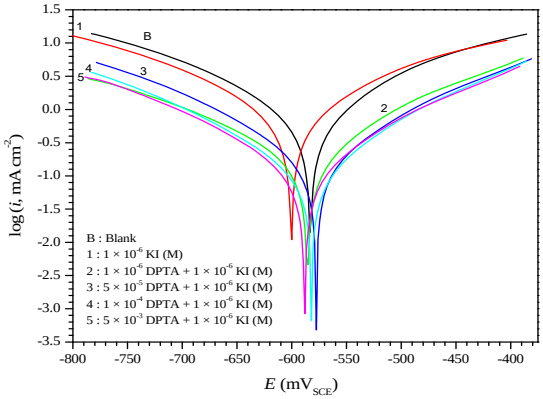

Figure 7: Polarization curves for carbon steel obtained in 1 M HCl solution and containing various concentrations of DPTA/KI

Table 2: Potentiodynamic electrochemical parameters for the corrosion of carbon steel in 1 M HCl solution in the absence and presence of investigated inhibitors at 298 K

DPTA Conc. (M)	KI Conc. (M)	$-E_{corr}$ mV(SCE)	i_{corr} (mA cm^{-2})	β_a (mV dec^{-1})	$-\beta_c$ (mV dec^{-1})	η_t (%)
0	0	583	1.847	221	228	–
1×10^{-6}	0	571	0.440	153	151	76.2
1×10^{-5}	0	575	0.378	131	141	79.6
1×10^{-4}	0	588	0.302	138	173	83.7
1×10^{-3}	0	573	0.258	135	139	86.0
0	1×10^{-6}	600	1.743	238	229	05.7
1×10^{-6}	1×10^{-6}	586	0.265	136	149	85.7
1×10^{-5}	1×10^{-6}	578	0.211	128	134	88.6
1×10^{-4}	1×10^{-6}	582	0.167	126	145	90.9
1×10^{-3}	1×10^{-6}	588	0.136	120	134	92.6

The inhibition efficiency, increased with DPTA concentration reaching a maximum value of 86% at 1×10^{-3} M. While the inhibition efficiency raise to 92.6% with addition 1×10^{-6} M KI to 1×10^{-3} M of DPTA inhibitor. The polarization curves also showed that addition of DPTA or DPTA/KI mixture decreases both cathodic and anodic current density. The cathodic hydrogen evolution reaction and anodic iron dissolution were inhibited after the addition of DPTA to the aggressive solution and this inhibition was more pronounced in the presence the iodide ions. Tafel lines are shifted to more negative and more positive potentials with respect to the blank curve by adding the investigated inhibitors. This behavior indicates that the undertaken additives act as mixed-type inhibitors [28]. The cathodic curves give rise to parallel lines indicating that the addition of the inhibitors to the 1 M HCl solution does not modify the hydrogen evolution mechanism (reduction of H^+ ions to H_2 through charge transfer). The inhibitor molecules are first adsorbed onto the steel surface and impedes by blocking the reaction sites of the steel surface. In this way, the surface area available for H^+ ions is decreased while the actual reaction mechanism remains unaffected [29]. In solutions with combination of DPTA/KI inhibitor, either higher coverage or thicker protective layer of the inhibitor on the surface was obtained. The corrosion potential E_{corr} values shifted very slightly with different inhibitor concentration, so it could also be deduced that the investigated inhibitors showed a mixed-type inhibitor [30].

3.3. Weight loss measurements

The corrosion rate (ν) obtained from weight loss measurements of carbon steel specimens after 24 h exposure to 1 M HCl solution with and without the addition of various concentrations of the investigated inhibitors are given in Table 3. The corrosion rate (mg cm^{-2} h^{-1}), surface coverage (θ) and inhibition efficiency (η_w) of each concentration were calculated using the following equations [31]:

$$\nu = \frac{\Delta W}{St} \quad (7)$$

$$\theta = \frac{\nu - \nu^0}{\nu} \quad (8)$$

$$\eta_w = \left(\frac{\nu - \nu^0}{\nu}\right) \times 100 \quad (9)$$

where ΔW is the average weight loss (mg), S is the surface area of specimens (cm^2), and t is the immersion time (h), ν and ν^0 are corrosion rates in the absence and presence of inhibitor, respectively.

Table 3: Corrosion parameters of carbon steel after 24 h immersion in 1 M HCl solution with and without various concentrations of investigated inhibitors

DPTA Conc. (M)	KI Conc. (M)	ν (mg cm^{-2} h^{-1})	θ	η_w (%)
0	0	5.994	–	–
1×10^{-6}	0	1.828	0.695	69.5
1×10^{-5}	0	1.778	0.703	70.3
1×10^{-4}	0	1.625	0.729	72.9
1×10^{-3}	0	0.839	0.860	86.0
0	1×10^{-6}	5.749	0.041	04.1
1×10^{-6}	1×10^{-6}	0.979	0.837	83.7
1×10^{-5}	1×10^{-6}	0.886	0.852	85.2
1×10^{-4}	1×10^{-6}	0.743	0.876	87.6
1×10^{-3}	1×10^{-6}	0.542	0.910	91.0

According to Table 3, the corrosion rate of carbon steel decreases with increasing DPTA concentration and decreases further in the presence of iodide ions combined with DPTA. These data also indicate that the inhibition efficiency rose up to 91% in the presence of (1×10^{-6} KI + 1×10^{-3} DPTA) compared with 4.1% and 86% for 1×10^{-6} KI and 1×10^{-3} DPTA, respectively. These indicate the synergistic inhibition effect between DPTA and KI.

3.4. Adsorption isotherm

The efficiency of organic compound as a successful corrosion inhibitor mainly depends on its adsorption ability on the metal surface. The adsorption isotherm can give valuable information on the interaction of inhibitor and metal surface. The surface coverage values (θ) of different concentrations of DPTA obtained from weight loss measurements were used to explain the best adsorption isotherm. A plot of C/θ versus C (Figure 8) gives a straight line with an average correlation coefficient of 0.9997 and a slope of nearly unity (1.1552) suggests that the adsorption of DPTA molecules obeys Langmuir adsorption isotherm, which can be expressed by the following equation [32]:

$$\frac{C}{\theta} = \frac{1}{K_{ads}} + C \quad (10)$$

where C is inhibitor concentration and K_{ads} is the equilibrium constant for the adsorption–desorption process.
The value K_{ads} calculated from the reciprocal of the intercept of isotherm line as 1.11×10^8 M^{-1}. The high value of the adsorption equilibrium constant reflects the high adsorption ability of this inhibitor on the carbon steel surface. The standard free energy of adsorption of the the inhibitor (ΔG^o_{ads}) on the carbon steel surface can be evaluated with the following equation;

$$\Delta G^o_{ads} = -RT\ln(55.5K_{ads}) \quad (11)$$

According to equation (11) the value of ΔG^o_{ads} was calculated as −56.78 kJ mol^{-1}. The negative value of standard free energy of adsorption indicates spontaneous adsorption of DPTA molecules on the carbon steel surface and also the strong interaction between inhibitor molecules and the metal surface [33].

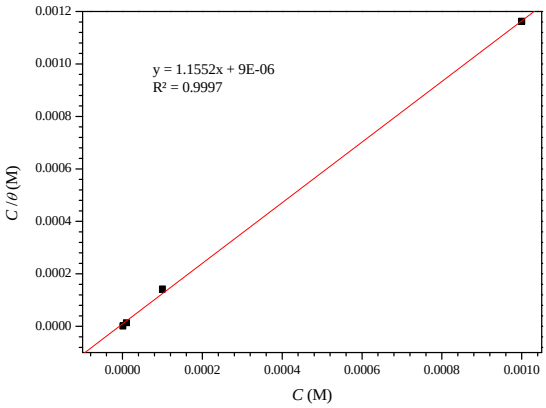

Figure 8: Langmuir adsorption plots of carbon steel in 1 M HCl solution containing various concentrations of DPTA

Generally, absolute values of ΔG^o_{ads} up to 20 kJ mol^{-1} are consistent with physisorption associated with electrostatic adsorption, while those around 40 kJ mol^{-1} or higher are associated with chemisorption as a result of the sharing or transfer of electrons from organic molecules to the metal surface to form a coordinate type of metal bonds [34]. Here, the calculated ΔG^o_{ads} values are higher than 40 kJ mol^{-1}, indicating that the adsorption mechanism of DPTA on the carbon steel in 1 M HCl solution is chemical adsorption.

3.5. Synergistic effect of iodide ions at different concentrations of DPTA

For describing the combined inhibition behavior of DPTA and KI the synergism parameter (S) was calculated from the data of weight loss, potentiodynamic and electrochemical impedance techniques and listed in Table 4 using the relationship given by Aramaki and Hackerman are [35]:

$$S = \frac{1-(\theta_1 + \theta_2)}{1-\theta_{1+2}} \quad (12)$$

where θ_1 is the surface coverage of DPTA, θ_2 is the surface coverage of KI and η_{1+2} is the surface coverage of DPTA/KI mixture.

As can be seen from Table 4, the surface coverage for solutions with DPTA/KI mixture exhibit higher values compared to solutions without KI. The iodide ions enhance the stability of the inhibitor on the metal surface by a co-adsorption mechanism, which may be either be competitive or cooperative [36]. In competitive adsorption the anion (iodide ion) and cation (protonated inhibitor) are adsorbed at different sites on the metal surface. While in cooperative, the anion is chemisorbed on the metal surface and the cation adsorbed on a layer of the anion [37].

Table 4: Synergism parameter at different concentrations of investigated inhibitors at 298 K

DPTA Conc. (M)	KI Conc. (M)	EIS		Tafel		W. Loss	
		θ	S	θ	S	θ	S
1×10^{-6}	0	0.580	–	0.76	–	0.69	–
1×10^{-5}	0	0.647	–	0.79	–	0.70	–
1×10^{-4}	0	0.663	–	0.83	–	0.72	–
1×10^{-3}	0	0.784	–	0.86	–	0.86	–
0	1×10^{-6}	0.081	–	0.05	–	0.04	–
1×10^{-6}	1×10^{-6}	0.794	1.34	0.85	1.2	0.83	1.01
1×10^{-5}	1×10^{-6}	0.811	1.11	0.88	1.2	0.85	1.06
1×10^{-4}	1×10^{-6}	0.858	1.36	0.90	1.1	0.87	1.06
1×10^{-3}	1×10^{-6}	0.869	1.04	0.92	1.1	0.91	1.10

Generally, synergism parameter implies antagonistic behavior at of S < 1, which may lead to competitive adsorption, whereas S > 1 indicates a synergistic effect (cooperative adsorption) [38]. Table 4 gives values of *S* which are more than unity, thereby suggesting that the enhanced inhibition efficiency caused by the addition of iodide ions to the inhibitors is due to only the synergistic effect.

3.6. Inhibition mechanism

The mechanism of the anodic dissolution of carbon steel in HCl is [39]:

$Fe + Cl^- \rightleftharpoons [FeCl^-]_{ads}$ (13)

$[FeCl^-]_{ads} \rightleftharpoons [FeCl]_{ads} + e^-$ (14)

$[FeCl]_{ads} \rightarrow [FeCl^+] + e^-$ (15)

$[FeCl^+] \rightleftharpoons Fe^{2+} + Cl^-$ (16)

The mechanism for cathodic hydrogen evolution is [40]:

$Fe + H^+ \rightleftharpoons [FeH^+]_{ads}$ (17)

$[FeH^+]_{ads} + e^- \rightarrow [FeH]_{ads}$ (18)

$[FeH]_{ads} + H^+ + e^- \rightarrow Fe + H_2$ (19)

The carbon steel surface is positively charged if the mechanism from the equation (16) is utilized. In this case, it would be difficult for the protonated DPTA molecules to approach the positively charged steel surface because of electrostatic repulsion. In the presence of iodide ions, the anions are adsorbed onto the steel surface, which allows the protonated DPTA molecules to easily approach the surface [41].

4. Conclusions

The inhibition behavior of DPTA and its synergistic effect with iodide ions for carbon steel in 1 M HCl has been studied. The following conclusions may be drawn:

1. From the all used techniques obtained in the presence of DPTA and iodide ions we conclude that there is a synergism between DPTA and iodide ions and the values of synergism parameter (*S*) are more than unity.
2. DPTA acts as a mixed-type inhibitor in the absence and presence of iodide ions.
3. The adsorption of DPTA on the carbon steel surface in 1 M HCl solution obeys Langmuir adsorption isotherm.

5. Acknowledgement

The authors are greatly thankful to the Egyptian Petroleum Research Institute (EPRI) fund and support.

References

[1] S. Saravanamoorthy, S. Velmathi, Prog. Org. Coat. 76 (2013) 1527–1535.
[2] N.D. Nam, Q.V. Bui, M. Mathesh, M.Y.J. Tan, M. Forsyth, Corros. Sci. 76 (2013) 257-266.
[3] N.D. Nam, A. Somers, M. Mathesh, M. Seter, B. Hinton, M. Forsyth, M.Y.J. Tan, Corros. Sci. 80 (2014) 128-138.
[4] Marian Bobina, Andrea Kellenberger, Jean-Pièrre Millet, Cornelia Muntean, Nicolae Vaszilcsin, Corros. Sci. 69 (2013) 389-395.
[5] Kosari, M.H. Moayed, A. Davoodi, R. Parvizi, M. Momeni, H. Eshghi, H. Moradi, Corros. Sci. 78 (2014) 138-150.
[6] Lubanski Fragoza-Mar, Octavio Olivares-Xometl, Marco A. Domínguez-Aguilar, Eugenio A. Flores, Paulina Arellanes-Lozada, Federico Jiménez-Cruz, Corros. Sci. 61 (2012) 171-184.
[7] Bin Xu, Wenzhong Yang, Ying Liu, Xiaoshuang Yin, Weinan Gong, Yizhong Chen, Corros. Sci. 78 (2014) 260–268.
[8] M. Behpour, S.M. Ghoreishi, N. Soltani, M. Salavati-Niasari, Corros. Sci. 51 (2009) 1073–1082.
[9] H. Keles, M. Keles, I. Dehri, O. Serindag, Osman Serindag, Colloid Surf. A 320 (2008) 138–145.
[10] H.A. Mohamed, A.A. Farag, B.M. Badran, Journal of Applied Polymer Science 117 (3), (2010) 1270–1278 .
[11] Xianghong Li, Shuduan Deng, Hui Fu, Guannan Mu, Corros. Sci. 51 (2009) 620–634.
[12] H.A. Mohamed, A.A. Farag, B.M. Badran, Eurasian Chemico-Technological Journal 10 (1), (2008) 67-77.
[13] X. Li, S. Deng, H. Fu, G. Mu, Corros. Sci. 52 (2010) 1167–1178.
[14] M.K. Pavithra, T.V. Venkatesha, K. Vathsala, K.O. Nayana, Corros. Sci. 52 (2010) 3811–3819.
[15] I.B. Obot, N.O. Obi-Egbedi, S.A. Umoren, Corros. Sci. 51 (2009) 276–282.
[16] M.A. Migahed, A.A. Farag, S.M. Elsaed, R. Kamal, H.A. El-Bary, Chem. Eng. Commun. 199 (2012) 1335-1356.

[17] M. Al-Sabagh, N. M. Nasser, Ahmed A. Farag, M. A. Migahed, A. M. F. Eissa, T. Mahmoud, Egyptian Journal of Petroleum 22 (2013) 101–116.
[18] M.A. Migahed, A.A. Farag, S.M. Elsaed, R. Kamal, M. Mostfa, H. Abd El-Bary, Mater. Chem. Phys. 125 (2011) 125–135.
[19] Ahmed A. Farag, M.A. Hegazy, Corros. Sci. 74 (2013) 168–177.
[20] Ahmed Y. Musa, Ramzi T.T. Jalgham, Abu Bakar Mohamad, Corros. Sci. 56 (2012) 176–183.
[21] K.F. Khaled, Appl. Surf. Sci. 252 (2006) 4120–4128.
[22] P Cao, R. Gu, Z. Tian, Langmuir 18 (2002) 7609–7615.
[23] M. Kissi,M. Bouklah, B. Hammouti, M. Benkaddour, Appl. Surf. Sci. 252 (2006) 4190-4197.
[24] C. Cao, Corros. Sci. 38(12) (1996) 2073–2082.
[25] Y. Fenga, S. Chenb, J. Youa, W. Guo, Electrochim. Acta 53 (2007) 1743–1753.
[26] D.D. Mac Donald, M.C.H. Mckubre, Modern Aspects of Electrochemistry, Plenum Press, New York (1982).
[27] Ahmed A. Farag, M.R. Noor El-Din, Corros. Sci. 64 (2012) 174–183.
[28] M.A. Quraishi, D. Jamal, Mater. Chem. Phys. 78 (2003) 608–613.
[29] M. Behpour, S.M. Ghreishi, N. Mohammadi, N. Soltani, M. Salavati-Niasari, Corros. Sci. 52 (2010) 4046–4057.
[30] Zhihua Tao, Shengtao Zhang, Weihua Li, Baorong Hou, Corros. Sci. 310 (2009) 2588–259.
[31] Bei Qian, Jing Wang, Meng Zheng, Baorong Hou, Corros. Sci. 75(2013) 184–192.
[32] W.H. Li, Q. He, S.T. Zhang, C.L. Pei, B.R. Hou, J. Appl. Electrochem. 38 (2008) 289–295.
[33] E. Cano, J.L. Polo, A. La Iglesia, J.M. Bastidas, Adsorption 10 (2004) 219–225.
[34] G. Quartarone, L. Ronchin, A. Vavasori, C. Tortato, L. Bonaldo, Corros. Sci. 64 (2012) 82–89.
[35] K. Aramaki, N. Hackerman, J. Electrochem. Soc. 116 (1969) 568–574.
[36] Q. Qu, Z. Hao, S. Jiang, L. Li, W. Bai, Mater. Corros. 59 (2008) 883–888.
[37] M. Bouklah, B. Hammouti, A. Aouniti, M. Benkaddour, A. Bouyanzer, Appl. Surf. Sci. 252 (2008) 6236–6242.
[38] Ahmed Y Musa, Abu Bakar Mohamad, Abdul Amir H. Kadhum, Mohd Sobri Takriff, Lim Tien Tien, Corros. Sci. 53(2011) 3672–3677.
[39] M. Behpour, S.M. Ghoreishi, N. Soltani, M. Salavati-Niasari, M. Hamadanian, A. Gandomi, Corros. Sci. 50 (2008) 2172–2181.
[40] R. Solmaz, Corros. Sci. 52 (2010) 3321–3330.
[41] Y. Feng, K.S. Siow, W.K. Teo, A.K. Hsieh, Corros. Sci. 41 (1999) 829–852.

Author Profile

Ahmed A. Farag received the B.Sc., Master and Ph.D. degrees in Chemistry from Science Faculty, Al-Azhar University/ Egypt in 2002, 2007 and 2011, respectively. I worked in National Research Center (NRC), Polymers and Pigments Department/Egypt until 2007. Now I am working in Egyptian Petroleum Research Institute (EPRI), Petroleum Applications Department/Egypt from 2007 until now.

Ismail M. Ibrahim, Asphalt Lab. Petroleum Applications Department, Egyptian Petroleum Research Institute (EPRI), 1 Ahmed El-Zomor St., Nasr City, 11727, Cairo, Egypt.